

A comparison of forest structural methods of semiarid mangrove species using a field-based approach

Francisco Flores-de-Santiago^{1*}, Francisco Flores-Verdugo²

ARTICLE INFO

Article history:

Received 08 August 2023

Accepted 06 December 2023

Published 27 February 2024

LEER EN ESPAÑOL:

<https://doi.org/10.7773/cm.v2024.3432>

CORRESPONDING AUTHOR

* E-mail: ffloresd@cmarl.unam.mx

¹ Instituto de Ciencias del Mar y Limnología, Unidad Académica Procesos Oceánicos y Costeros, Universidad Nacional Autónoma de México, 04510 Ciudad Universitaria, Ciudad de México, Mexico.

² Instituto de Ciencias del Mar y Limnología, Unidad Académica Mazatlán, Universidad Nacional Autónoma de México, 82040 Mazatlán, Sinaloa, Mexico.

ABSTRACT. The data obtained from field-based forest inventories, mainly basal area and stem density, are relevant for the analysis of aboveground biomass and forest fragmentation. Due to its persistently flooded ground, fieldwork in mangrove forests is time-consuming and complicated. Since mangroves are sensitive to the effects of climate change, selecting a reliable field method is of utmost importance. To this end, we analyzed 4 mangrove classes: *Rhizophora mangle* (RM), *Laguncularia racemosa* (LR), *Avicennia germinans* (AG), and AG shrub. We georeferenced and counted all mangrove stems within four 0.04 ha (20 × 20 m square). We analyzed data from 3 circular area plots and the plotless point-centered quarter method (PCQM) based on the original square plots. Depending on the mangrove class, PCQM overestimated basal area by up to 34% and stem density by 21%. The 3 circular plot surveys underestimated basal area from -1% to -29% and stem density from -3 to -25%. Based on the results, we suggest using a circular plot of 0.04 ha ($r = 11.28$ m) in less dense forests (RM and AG) and a circular plot of 0.015 ha ($r = 6.9$ m) with forest densities greater than 3,500 stems/ha (LR and AG shrub). The advantages of using the circular plot approach over PCQM are that mangrove inventories can be quantified quickly and do not require a minimum number of sampling points.

Key words: point-centered quarter method, circular plots, basal area, stem density.

INTRODUCTION

Mangrove forests are composed of trees and shrubs that thrive in intertidal zones between tropical and subtropical latitudes. These forests provide ecosystem services such as protecting against coastal erosion and providing nursery grounds for commercial species (Ximenes et al. 2023). Field-based mangrove forest variables, such as basal area and stem density, are of utmost importance for estimating structural complexity and aboveground biomass (Tran et al. 2022) and corroborating data from remote sensors (Vizcaya-Martínez et al. 2022).

The differences among mangrove field-based inventory variables depend on the species, geographic region, and forest type (Wang et al. 2018). For example, mangrove

forests in tropical zones with higher annual rainfall rates tend to present higher basal areas and less stem density than mangroves in arid or semiarid regions (Valderrama-Landeros et al. 2022). The logistics of fieldwork in mangrove forests are much more complicated and time-consuming than in other terrestrial forests (Salum et al. 2020). For instance, the coastal environments where mangroves thrive are arduous for fieldwork, mainly due to tidal fluctuations and muddy soil (Ferreira et al. 2022). In addition, the soil of degraded mangrove forests tends to be less compact than that of mangroves living under optimal conditions, increasing the difficulty of fieldwork (Flores-Verdugo et al. 2015). Thus, it is necessary to identify the ideal method to efficiently carry out mangrove field-based surveys for each species within a mangrove forest.

Open Access

Online ISSN: 2395-9053

Screened via Similarity Check powered by iThenticate

<https://doi.org/10.7773/cm.v2024.3432>



This is an Open Access article distributed under the terms of the [Creative Commons Attribution 4.0 International License \(CC BY 4.0\)](https://creativecommons.org/licenses/by/4.0/), which allows you to share and adapt the work, as long as you give appropriate credit to the original author(s) and the source, provide a link to the Creative Commons license, and indicate if changes were made. Figures, tables, and other elements in the article are included in the article's CC BY 4.0 license, unless otherwise indicated. You must seek permission from the copyright holder for use of material not covered by this license. The journal title is protected by copyrights owned by Universidad Autónoma de Baja California, and the journal title and logo are not subject to this license.

There are several ways to perform field-based inventories, including distance-based techniques (plotless approaches), such as the point-centered quarter method (PCQM), and area-based approaches (square and circular plots). Overall, fixed square plots of up to 0.16 ha (40×40 m) in which all stems within the area are counted are generally preferred for long-term monitoring purposes (Villeda-Chávez et al. 2018, Valderrama-Landeros et al. 2020). However, since these field-based observations are restricted to only a few permanently installed plots, the acquired data are spatially limited (Flores-de-Santiago et al. 2023). For this reason, when spatially analyzing a mangrove system to corroborate biomass estimations from remote sensors, including synthetic aperture radar and unmanned aerial vehicles, or existing metrics, such as leaf area indices from the literature, it is better to cover multiple small stations such as circular plots (Flores-de-Santiago et al. 2013, 2020). The PCQM approach utilizes transects that traverse forests, thereby eliminating the need to designate specific sampling areas. However, the effectiveness of this method depends on the number of stations with transects. Moreover, the size of the forest may not be sufficiently large for PCQM.

The objective of this study was to determine the degree of error among traditional field-based survey methods for mangrove forests in a semiarid system of the Gulf of California using a field-based approach. The working hypothesis was that the optimal method would depend on the stem density of the mangrove species. Due to the gaps within the plots, we expected an inverse estimation error relationship between stem density and basal area.

MATERIALS AND METHODS

Study area

The Urias coastal lagoon (Fig. 1) is a small (18 km^2), shallow (<4 m depth) water body located on the semiarid eastern coast of the Gulf of California, Mexico ($23^\circ 09' 06''$ N, $106^\circ 19' 57''$ W). Three mangrove species partially border the coastal lagoon: *Rhizophora mangle* L. (RM), *Laguncularia racemosa* (L.) Gaertn (LR), and *Avicennia germinans* (L.) L. (AG) (Valderrama-Landeros et al. 2018, 2021). The short rainy season and tendency of the coastal lagoon to exhibit hypersaline conditions have resulted in extensive shrub-like AG mangrove communities in areas with low water exchange (Flores-Verdugo et al. 2015).

Square plot

We collected structure data in the field from 20–28 February 2022 from 4 monospecific mangrove forest classes of RM, LR, AG, and AG shrub along the southern portion of the Urias coastal lagoon. We installed a rope perimeter surrounding a square area (40×40 m, 0.16 ha) in each mangrove forest class as described by Villeda-Chávez et al. (2018). We

first determined the structure of the area to be analyzed in each square plot by calculating the position of each stem with a portable laser and measuring its diameter at breast height (DBH) with diametral tape. We subdivided each square plot into 4 sections (20×20 m) for statistical analysis.

Plotless PCQM

We installed 3 permanent 40-m line transects in the 4 monospecific mangrove class plots. We divided each sampling point along the line into 4 quadrants according to the cardinal directions (Cintrón and Schaeffer-Novelli 1984). For each quadrant, we measured the distance to the nearest mangrove stem. In other words, we collected 4 distance measurements with their corresponding DBH per sampling point. The same stem could not be measured twice between 2 consecutive sampling points.

Circular plot method

According to the methods of Kovacs et al. (2010), we counted the stems within 3 circular plots measuring 0.04 ha ($r = 11.28$ m), 0.03 ha ($r = 9.77$ m), and 0.015 ha ($r = 6.9$ m) for each monospecific mangrove class. In the case of LR and AG shrub, some stems exhibited diameters less than 2.5 cm, a value which is generally not considered in mangrove structure studies. For this reason, LR and AG shrub were analyzed using (1) the total number of stems (i.e., all stems) regardless of their DBH and (2) stems with DBH values greater than 2.5 cm. We calculated the basal areas (m^2/ha) and densities (stems/ha) for all the aforementioned methods.

Statistical analyses

To determine whether significant differences ($P < 0.05$) in basal area and stem density existed among the 4 sampling methods, we conducted an unbalance one-way ANOVA using the arithmetic mean, standard deviation, and number of samples per method (Sokal and Rohlf 2012). We used Tukey's post-hoc test to evaluate significant differences. All analyses were conducted in Matlab v. R2016a. We calculated the coefficient of variation (CV), which is the ratio of the standard deviation to the mean, for basal area and stem density. We estimated the error percentage for the 4 sampling methods by subtracting the total basal area and stem density from the main square plot.

RESULTS

All mangrove classes presented some multi-stemmed trees (Fig. 2). For the square plot method, the spatial distribution of the stems varied according to the species; for example, the RM forest presented low density (444 stems/ha), scattered trees, and low basal area ($4.8 \text{ m}^2/\text{ha}$) (Table 1). The LR forest exhibited a higher density (3,225 stems/ha) of multi-stem

trees with a relatively high basal area (13.4 m²/ha). In contrast, the AG forest contained scattered trees (1,069 stems/ha) with a small basal area (5.7 m²/ha). Finally, AG shrub presented high density (6,500 stems/ha) and a basal area of 14.6 m²/ha distributed in dense clusters and spaces among the analyzed stems. Due to the high density of smaller-sized stems, LR and AG shrub exhibited different densities when considering all data but with a basal area that remained relatively unchanged. For example, the LR forest increased from 3,225 to 4,500 stems/ha, and its basal area increased from 13.4 to 13.7 m²/ha. On the other hand, the AG density in AG shrub increased from 6,269 to 6,500 stems/ha, while its basal area only increased from 14.5 to 14.6 m²/ha.

The time required for 4 people to complete a field-based mangrove inventory within a square plot (0.16 ha) was 1 h and 20 min for RM, 1 h for LR, 20 min for AG, and 2 h for AG shrub. The DBH distribution of the 4 mangrove classes revealed noticeable differences. For example, most RM stems exhibited DBH frequencies between 8 and 10 cm, followed by a second group composed of frequencies between 12 and 14 cm. The LR forest exhibited high density for stems less than 4 cm. The AG forest exhibited a normal distribution with frequencies between 4 and 6 cm, while AG shrub presented much higher densities between 4 and 6 cm.

The RM class showed no significant differences in basal area ($F_{(4,116)} = 2.6, P = 0.04$) and stem density ($F_{(4,116)} = 4.1, P = 0.004$) among the 4 sampling methods when compared

with those of the square method. The 0.04-ha circle and PCQM approaches resulted in the smallest estimated error. The PCQM approach also resulted in the lowest CV for basal area and stem density; however, PCQM required more time to complete than the circular area plot method. The LR class (DBH > 2.5 cm) showed significant differences among the methods in terms of basal area ($F_{(4,799)} = 184.2, P = 0.0$), but the post-hoc analysis revealed no significant differences between the 0.04-ha and 0.03-ha circles ($P = 0.43$). Nonetheless, all methods showed significant differences ($F_{(4,799)} = 145.9, P = 0.0$) in stem density for the LR class. Moreover, PCQM showed the highest basal area and stem density errors, and we recorded the lowest estimated errors with the 0.015-ha circle.

The AG class showed significant differences in both basal area ($F_{(4,285)} = 25.1, P = 0.0$) and stem density ($F_{(4,285)} = 21.3, P = 0.0$), but the post-hoc analysis indicated that there were no significant differences between the square plot and PCQM ($P = 1$) and the circular plot of 0.04 ha ($P = 0.98$) for both variables. All methods showed significant differences in basal area ($F_{(4,1543)} = 41.3, P = 0.0$) and stem density ($F_{(4,1543)} = 244.2, P = 0.0$) in the AG shrub class. However, we estimated a minimum error for both variables within the circular plot of 0.015 ha. The statistical results for LR (all stems) and AG shrub (all stems) did not vary compared to the results of the previous analyses with stems larger than 2.5 cm.

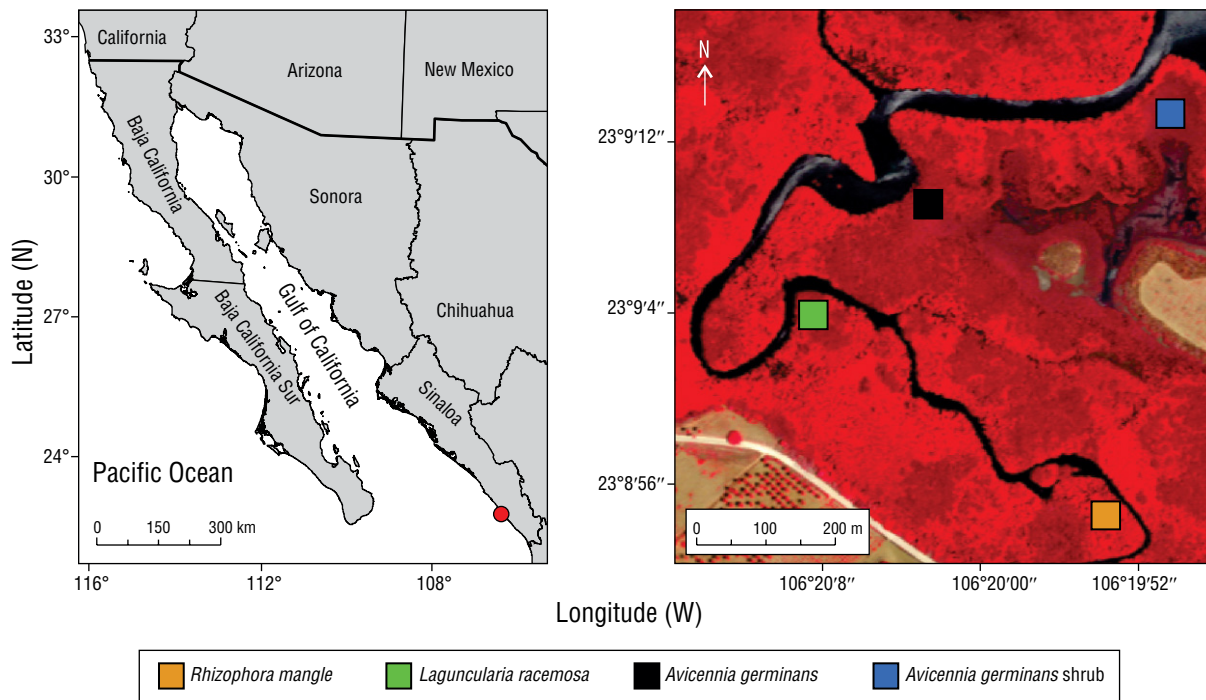


Figure 1. Locations of the field-based mangrove inventories in the southwestern Gulf of California in the Mexican Pacific. The bold line indicates the USA–Mexico international border, and the red circle depicts the location of the Urias system. Each colored rectangle indicates the survey area of 0.16 ha of each mangrove class over a false-color composite (near infrared, red, green) GeoEye image.

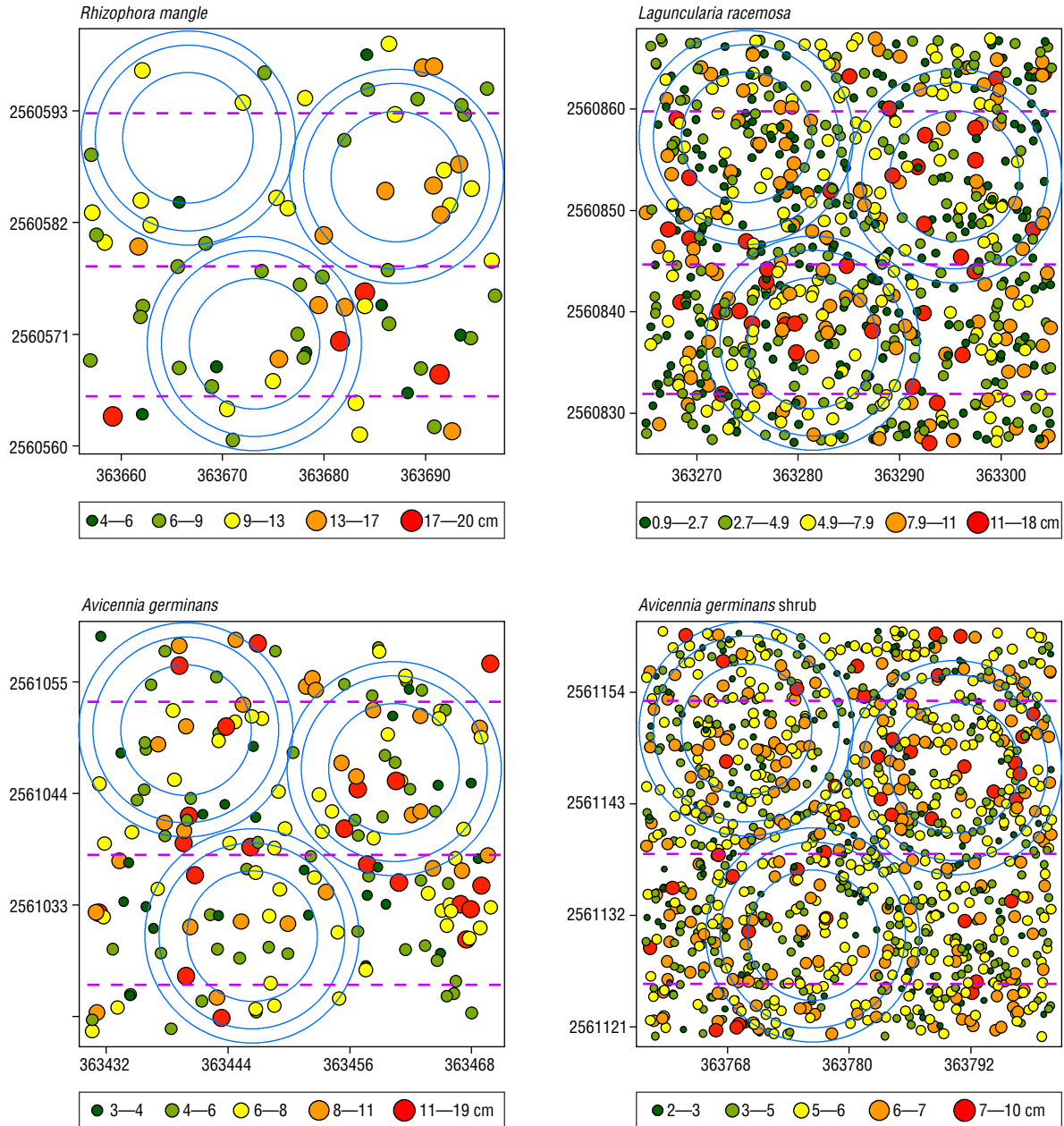


Figure 2. The spatial distribution of mangrove stems according to the diameter at breast height (DBH; small circles) measured for the 4 mangrove classes (*Rhizophora mangle*, *Laguncularia racemosa*, *Avicennia germinans*, and *Avicennia germinans shrub*). Each square measured 40 × 40 m. The 3 blue circles indicate the locations of the circular plots (0.04, 0.03, and 0.015 ha). The purple lines indicate the locations of the 3 point-centered quarter method (PCQM) transects.

DISCUSSION

Given that costs are high, surveying an entire 0.16-ha plot may not be ideal except for continuous or long-term monitoring (Villeda-Chávez et al. 2018). It is important to select the easiest, fastest, and most reliable method to obtain field-based mangrove structural data with as few people as possible, especially when working in large areas with many field stations (Flores-Verdugo et al. 1992). The circular plot

method can be conducted quickly, while PCQM is usually more labor-intensive and requires at least one individual tree in each quarter. On the other hand, PCQM depends on a linear or semi-linear transect based on the configuration of the mangrove forest (Flores-Verdugo et al. 1990). In our analyses, the maximum number of PCQM points varied as follows: 5 in RM, 10 in LR, 8 in AG, and 14 in AG shrub. Hence, covering the minimum number of 20 sampling points along the transect for PCQM (Cottam and Curtis 1956) is often impossible

Table 1. Summary of basal area and stem density using the sampling methods in the mangrove classes of *Rhizophora mangle* (RM), *Laguncularia racemosa* (LR), *Avicennia germinans* (AG), and AG shrub.

Mangrove class and method	Basal area (m ² /ha)	Basal area CV	Density (stems/ha)	Density CV	Number of stems	Basal area error (%)	Density error (%)
RM–Square plot (0.04 ha)	4.8 ± 1.7	0.4	444 ± 120	0.3	72		
RM–PCQM	4.3 ± 0.9	0.2	385 ± 74	0.2	20	–11	–13
RM–Circular plot (0.04 ha)	4.3 ± 3.6	0.9	378 ± 214	0.6	13 ± 4	–11	–15
RM–Circular plot (0.03 ha)	3.7 ± 1.7	0.5	333 ± 145	0.4	10 ± 4	–23	–25
RM–Circular plot (0.015 ha)	3.4 ± 1.2	0.4	333 ± 101	0.3	6 ± 3	–29	–25
LR (>2.5 cm)–Square plot (0.04 ha)	13.4 ± 0.5	0.0	3,225 ± 172	0.1	516		
LR (>2.5 cm)–PCQM	17.9 ± 3.0	0.2	3,909 ± 447	0.1	40	34	21
LR (>2.5 cm)–Circular plot (0.04 ha)	12 ± 1.6	0.1	2,833 ± 427	0.2	113 ± 17	–10	–12
LR (>2.5 cm)–Circular plot (0.03 ha)	12.3 ± 2.1	0.2	2,933 ± 416	0.1	88 ± 12	–8	–9
LR (>2.5 cm)–Circular plot (0.015 ha)	13.5 ± 1.3	0.1	3,445 ± 234	0.1	47 ± 6	1	7
AG–Square plot (0.04 ha)	5.7 ± 0.1	0.0	1,069 ± 24	0.0	172		
AG –PCQM	5.7 ± 1.4	0.2	1,076 ± 275	0.3	32	1	1
AG –Circular plot (0.04 ha)	5.8 ± 2.0	0.4	1,033 ± 34	0.0	37 ± 4	2	12
AG –Circular plot (0.03 ha)	5.1 ± 0.7	0.1	1,200 ± 241	0.2	31 ± 1	–11	–3
AG –Circular plot (0.015 ha)	4.4 ± 0.8	0.2	917 ± 101	0.1	18 ± 4	–23	–14
AG shrub (>2.5 cm)–Square plot (0.04 ha)	14.5 ± 1.1	0.1	6,269 ± 499	0.1	1027		
AG shrub (>2.5 cm)–PCQM	13 ± 1.7	0.1	5,467 ± 416	0.1	56	–10	–13
AG shrub (>2.5 cm)–Circular plot (0.04 ha)	16.5 ± 7.0	0.4	5,408 ± 413	0.1	216 ± 17	14	–14
AG shrub (>2.5 cm)–Circular plot (0.03 ha)	13.2 ± 1.5	0.1	555 ± 329	0.1	167 ± 10	–9	–11
AG shrub (>2.5 cm)–Circular plot (0.015 ha)	14 ± 0.3	0.0	5,720 ± 394	0.1	82 ± 6	–1	–9
LR (all stems)–Square plot (0.04 ha)	13.7 ± 0.5	0.0	4,500 ± 225	0.1	720		
LR (all stems)–PCQM	15.2 ± 2.8	0.2	3,909 ± 447	0.1	40	11	–13
LR (all stems)–Circular plot (0.04 ha)	12.3 ± 1.6	0.1	4,100 ± 541	0.1	164 ± 22	–10	–9
LR (all stems)–Circular plot (0.03 ha)	12.7 ± 2.1	0.2	4,267 ± 367	0.1	128 ± 11	–8	–5
LR (all stems)–Circular plot (0.015 ha)	13.8 ± 1.4	0.1	4,334 ± 757	0.2	65 ± 11	1	–4
AG shrub (all stems)–Square plot (0.04 ha)	14.6 ± 1.1	0.1	6,500 ± 497	0.1	1040		
AG shrub (all stems)–PCQM	14.1 ± 0.3	0.0	5,720 ± 394	0.1	56	–3	–12
AG shrub (all stems)–Circular plot (0.04 ha)	16.6 ± 7.0	0.4	5,608 ± 388	0.1	224 ± 16	14	–14
AG shrub (all stems)–Circular plot (0.03 ha)	13.3 ± 1.5	0.1	5,789 ± 334	0.1	174 ± 10	–9	–11
AG shrub (all stems)–Circular plot (0.015 ha)	13.1 ± 1.7	0.1	5,733 ± 437	0.1	86 ± 7	–10	–12

CV: Coefficient of variation

PCQM: Point-Centered Quarter Method

because the forest likely includes other species. For example, selecting several parallel, field-based circular plots may be a more feasible option, as the fringe mangroves of the Urias system extend approximately 50 m from the edge of the tidal channel.

Regarding basal area and stem density, our results indicate differences between PCQM and the 3 circular plots, except for the RM class. The PCQM method overestimated the basal area by 34% in some mangrove classes, which was likely the result of high stem density and sparse distributions (e.g., LR class). Hijbeek et al. (2013) also reported large stem density differences when employing PCQM at other sites due to errors that arose when 2 mangrove classes were mixed within the same transect. Our semiarid mangrove classes exhibited a high stem density that could result in similar errors. However, other mangrove conditions exist in tropical areas with much larger basal areas and lower stem densities (Kovacs et al. 2010). Thus, the PCQM method could be suitable in those large mangrove forests, as Araújo and Shideler (2019) and Dookie et al. (2022) suggested.

The distribution and composition of our mangrove classes were similar to those found in other regions of the Mexican Pacific under arid and semiarid conditions (Kovacs et al. 2013). Therefore, the results of this field-based mangrove inventory analysis can be used in other sites in this region or in other arid or semiarid zones worldwide. The method that yielded the best results was the circular plot of 0.04 ha in places where tree density was less than 3,500 stems/ha (RM and AG) and the circular plot of 0.015 ha, which contained higher tree density. Moreover, the required sampling time directly increased with the amount of surveyed area (LR and AG shrub). However, using sample area plots may not be feasible in field-based inventories when evaluating sparse or open-canopy mangrove forests, such as those found in degraded environments (Villeda-Chávez et al. 2018). Therefore, selecting the optimal method will benefit field-based estimates of aboveground biomass with allometric equations designed for each mangrove species in natural and rehabilitated forests. Moreover, our results provide critical additional information to improve mangrove restoration and rehabilitation strategies and provide complementary information to develop conservation policies (Ávila-Flores et al. 2020). Further validation of this structural method comparison is needed in other mangrove sites with diverse physiognomic compositions, including petenes (karst soil), overwashed areas (e.g., islands), and riparian systems. The results of additional validation studies will provide a more comprehensive understanding of the applicability of the methods to different mangrove ecosystems.

ACKNOWLEDGMENTS

The research leading to these results received funding from *Programa de Apoyo a Proyectos de Investigación e Innovación Tecnológica* (PAPIIT, UNAM, Mexico) under

grant agreements IA100218 and No IA100521. Partial financial support was received from *Instituto de Ciencias del Mar y Limnología* (UNAM, Mexico) under grant ICML–622. L.A. Díaz-Lara and R. Cruz-García assisted with field-based data collection. D. Daniel-Ramírez processed part of the results. G. Feher edited the English text. M. Reguero reviewed the Spanish text and the taxonomic names of the species.

REFERENCES

- Araújo RJ, Shideler GS. 2019. Un paquete de R para el cálculo de parámetros estructurales de bosques de manglar utilizando métodos con y sin parcelas. 25(1):e2511696. <http://dx.doi.org/10.21829/myb.2019.2511696>
- Ávila-Flores G, Juárez-Mancilla J, Hinojosa-Arango G, Cruz-Chávez P, López-Vivas JM, Arizpe-Covarrubias O. 2020. A practical index to estimate mangrove conservation status: The forests from La Paz, Mexico as a case study. *Sustainability*. 12(3):858. <http://dx.doi.org/10.3390/su12030858>
- Cintrón G, Schaeffer-Novelli Y. 1984. Methods for studying mangrove structure. In: Snedaker SC, Snedaker JG (eds.), *The mangrove ecosystem: research methods*. Paris: Unesco. p. 91-113.
- Cottam G, Curtis JT. 1956. The use of distance measures in phytosociological sampling. *Ecol*. 37(3):451-460. <http://dx.doi.org/10.2307/1930167>
- Dookie S, Jaikishun S, Ansari AA. 2022. A comparative study of mangroves in degraded, natural, and restored ecosystems in Guyana. *Biodivers*. 23(2):40-48. <https://doi.org/10.1080/14888386.2022.2107570>
- Ferreira AC, Morais Freire FA, Machado Rodrigues JV, Arruda Bezerra LE. 2022. Mangrove recovery in semiarid coast shows increase of ecological processes from biotic and abiotic drivers in response to hydrological restoration. *Wetlands*. 42:80. <https://doi.org/10.1007/s13157-022-01603-0>
- Flores-de-Santiago F, Rodríguez-Sobreyra R, Álvarez-Sánchez LF, Valderrama-Landeros L, Amezcua F, Flores-Verdugo F. 2023. Understanding the natural expansion of white mangrove (*Laguncularia racemosa*) in an ephemeral inlet based on geomorphological analysis and remote sensing data. *J Environ Manage*. 338:117820. <https://doi.org/10.1016/j.jenvman.2023.117820>
- Flores-de-Santiago F, Valderrama-Landeros L, Rodríguez-Sobreyra R, Flores-Verdugo F. 2020. Assessing the effect of flight altitude and overlap on orthoimage generation for UAV estimates of coastal wetlands. *J Coastal Conserv* 24:35. <https://doi.org/10.1007/s11852-020-00753-9>
- Flores-de-Santiago F, Kovacs JM, Lafrance P. 2013. An object-oriented classification method for mapping mangroves in Guinea, West Africa, using multipolarized ALOS PALSAR L-band data. *Int J Remote Sens*. 34:563-586. <http://dx.doi.org/10.1080/01431161.2012.715773>
- Flores-Verdugo F, González-Farías F, Ramírez-Flores O, Amezcua-Linares F, Yáñez-Arancibia A, Alvarez-Rubio M, Day JW. 1990. Mangrove ecology, aquatic primary productivity, and fish community dynamics in the Teacapán-Agua Brava lagoon-estuarine system (Mexican Pacific). *Estuaries*. 13:219-230. <https://doi.org/10.2307/1351591>
- Flores-Verdugo F, González-Farías F, Zamorano DS, Ramirez-García P. 1992. Mangrove ecosystems of the Pacific coast of Mexico: Distribution, structure, litterfall, and detritus

- dynamics. *Physiol Ecol.* 17:269-288.
<http://dx.doi.org/10.1016/B978-0-08-092567-7.50023-4>
- Flores-Verdugo F, Zebadua-Penagos F, Flores-de-Santiago F. 2015. Assessing the influence of artificially constructed channels in the growth of afforested black mangrove (*Avicennia germinans*) within an arid coastal region. *J Environ Manage.* 160:113-120.
<http://dx.doi.org/10.1016/j.jenvman.2015.06.024>
- Hijbeek R, Koedam N, Khan MNI, Kairo JG, Schoukens J, Dahdouh-Guebas F. 2013. An Evaluation of Plotless Sampling Using Vegetation Simulations and Field Data from a Mangrove Forest. *PLoS ONE.* 8:e67201.
<http://dx.doi.org/10.1371/journal.pone.0067201>
- Kovacs JM, Flores-de-Santiago F, Bastien J, Lafrance P. 2010. An assessment of mangroves in Guinea, West Africa, using a field and remote sensing based approach. *Wetlands.* 30:773-782.
<http://dx.doi.org/10.1007/s13157-010-0065-3>
- Kovacs JM, Jiao X, Flores-de-Santiago F, Zhang C, Flores-Verdugo F. 2013. Assessing relationships between Radarsat-2 C-band and structural parameters of a degraded mangrove forest. *Int J Remote Sens.* 34:7002-7019.
<http://dx.doi.org/10.1080/01431161.2013.813090>
- Salum RB, Souza-Filho PWM, Simard M, Silva CA, Fernandes MEB, Cougo MF, Junior WN, Rogers K. 2020. Improving mangrove aboveground biomass estimates using LiDAR. *Estuarine Coastal Shelf Sci.* 236:106585.
<https://doi.org/10.1016/j.ecss.2020.106585>
- Sokal RR, Rohlf FJ. 2012. *Biometry*, 4th Ed. New York (NY): WH Freeman and Company. 960 p.
- Tran TV, Reef R, Zhu X. 2022. A review of spectral indices for mangrove remote sensing. *Remote Sens.* 14(19):4868.
<https://doi.org/10.3390/rs14194868>
- Valderrama-Landeros L, Flores-Verdugo F, Flores-de-Santiago F. 2022. Assessing the coastal vulnerability by combining field surveys and the analytical potential of CoastSat in a highly impacted tourist destination. *Geographies* 2:642-656.
<https://doi.org/10.3390/geographies2040039>
- Valderrama-Landeros L, Flores-Verdugo F, Rodríguez-Sobreyra R, Kovacs JM, Flores-de-Santiago F. 2021. Extrapolating canopy phenology information using Sentinel-2 data and the Google Earth Engine platform to identify the optimal dates for remotely sensed image acquisition of semiarid mangroves. *J Environ Manage.* 279:111617.
<https://doi.org/10.1016/j.jenvman.2020.111617>
- Valderrama-Landeros L, López-Portillo J, Velázquez-Salazar S, Alcántara-Maya JA, Troche-Souza C, Rodríguez-Zúñiga MT, Vázquez-Balderas B, Villeda-Chavez E, Cruz-López MI, Ressler R. 2020. Regional distribution and change dynamics of mangroves in Mexico between 1970/80 and 2015. *Wetlands.* 40:1295-1305.
<https://doi.org/10.1007/s13157-020-01299-0>
- Valderrama-Landeros L, Flores-de-Santiago F, Kovacs JM, Flores-Verdugo F. 2018. An assessment of commonly employed satellite-based remote sensors for mapping mangrove species in Mexico using an NDVI-based classification scheme. *Environ Monit Assess.* 190:23.
<https://doi.org/10.1007/s10661-017-6399-z>
- Villeda-Chávez E, Lara AL, González-Zamorano P, Rubio EA, Valderrama L, Ramírez-García P, García-Calva L, Argüello-Velázquez J, Cruz-López MI. 2018. Muestreo de variables estructurales. In: Rodríguez-Zúñiga MT, Villeda-Chávez E, Vázquez-Lule AD, Bejarano M, Cruz-López MI, Olguín M, Villela-Gaytán SA, Flores R (eds.), *Métodos para la caracterización de los manglares mexicanos: un enfoque espacial multiescala*. Ciudad de México (Mexico): Comisión Nacional para el Conocimiento y Uso de la Biodiversidad. p. 71-130.
- Vizcaya-Martínez DA, Flores-de-Santiago F, Valderrama-Landeros L, Serrano D, Rodríguez-Sobreyra R, Álvarez-Sánchez LF, Flores-Verdugo F. 2022. Monitoring detailed mangrove hurricane damage and early recovery using multisource remote sensing data. *J Environ Manage.* 320:115830.
<https://doi.org/10.1016/j.jenvman.2022.115830>
- Wang M, Cao W, Guan Q, Wu G, Wang F. 2018. Assessing changes of mangrove forest in a coastal region of southeast China using multi-temporal satellite images. *Estuarine Coastal Shelf Sci.* 207:283-292.
<https://doi.org/10.1016/j.ecss.2018.04.021>
- Ximenes AC, Cavanaugh KC, Arvor D, Murdiyarto D, Thomas N, Arcoverde GFB, Bispo PC, Stocken TV. 2023. A comparison of global mangrove maps: Assessing spatial and bioclimatic discrepancies at poleward range limits. *Sci Total Environ.* 860:160380.
<http://dx.doi.org/10.1016/j.scitotenv.2022.160380>